

# Influence of copper hexacyanoferrate film thickness on the electrochemical properties of self-assembled 3-mercaptopropyl gold electrode and application as a hydrazine sensor

Andréia de Morais · Fábio L. Pissetti ·  
Alzira M. S. Lucho · Yoshitaka Gushikem

Received: 25 June 2009 / Revised: 14 October 2009 / Accepted: 20 October 2009 / Published online: 10 November 2009  
© Springer-Verlag 2009

**Abstract** A copper hexacyanoferrate film was obtained on a modified electrode prepared by self-assembly of 3-mercaptopropyltrimethoxysilane on a gold surface. The film thickness was controlled using a layer-by-layer technique to tune the electrocatalytic properties of the electrode. Two electrodes with different hexacyanoferrate film thicknesses were prepared via three immersions (AuS/CuHCF3) and six immersions (AuS/CuHCF6) of the film in the precursor solutions. Cyclic voltammetry data were obtained to determine the adequate film thickness. Scanning electron microscopy images showed a roughness increase due to the growth of the film thickness at the electrode surface. Electrochemical impedance spectroscopy showed distinct behavior for the two electrodes prepared; while diffusion and charge transfer processes can be observed in both electrodes, an additional capacitive process at intermediary frequencies was observed for the AuS/CuHCF6 electrode. The charge transfer resistance ( $R_{ct}$ ) for the AuS/CuHCF3 electrode ( $19.6 \Omega \text{ cm}^2$ ) was lower than for AuS/CuHCF6 ( $27.9 \Omega \text{ cm}^2$ ) due to the hexacyanoferrate film thickness, since the charge transfer process demands the simultaneous diffusion of  $\text{K}^+$  into the surface. Cyclic voltammetry was used to evaluate the application of

the AuS/CuHCF3 electrode as an electrochemical sensor, revealing a linear correlation for hydrazine concentrations.

**Keywords** 3-mercaptopropyltrimethoxysilane · Gold electrode · Self-assembly · Copper hexacyanoferrate

## Introduction

In recent years, an increasing interest in producing interfaces with well-defined composition, structure, orientation, thickness, and chemical functionality has been observed. Specific modification of surfaces is a major challenge in the preparation of function-oriented materials. Of the various procedures employed to obtain these types of materials, the layer-by-layer method has been most often used to prepare different types of self-organized systems [1–4].

The literature reports that gold interacts strongly with sulfur, forming a stable bond between the two species; as a consequence, a simple surface modification can be achieved. The alkoxy silane molecular layers have a significant advantage over other types of silanes due to the possibility of acting as a bifunctional group. The formation of self-assembled layers of mercaptopropyltrimethoxysilane on gold increases the electrode-film adhesion via thiol group interaction on both substrate and film. To obtain a tridimensional network on the surface electrode, the sol-gel method starting from a solution where hydrolysis is carried out under optimal conditions and condensation occurs very slowly, is an interesting approach. In these conditions, sulfur bonds with gold at the surface electrode and the self-condensation of Si-OH groups form

A. de Morais · F. L. Pissetti · A. M. S. Lucho (✉)  
Departamento de Ciências Exatas,  
Universidade Federal de Alfenas,  
37130-000 Alfenas, Minas Gerais, Brazil  
e-mail: lucho@unifal-mg.edu.br

Y. Gushikem  
Instituto de Química, Universidade Estadual de Campinas,  
C. Postal 6154,  
13084-971 Campinas, São Paulo, Brazil

the network. The gold is covered by the siloxane framework and presents free SH groups at the new electrode surface. The self-assembly of different electroactive layers on a substrate can be used to tune the electrocatalytic properties of the electrode [5–7].

Anionic electroactive complexes, especially Prussian blue analogs, have been extensively studied due their interesting electrocatalytic, electrochromic, ion exchange, ion sensing, and photomagnetic properties. Hexacyanoferrate ion is a chemical species known to have electron mediator properties and can be adsorbed on the surface of a solid by a simple ion exchange reaction to obtain a chemically modified electrode. A wide range of substrates were used to obtain this type of electrode including gold, platinum, glassy carbon, ceramic carbon, and fiber carbon. These compounds are usually prepared by chemical and electrochemical methods [8–11].

Many reports in the literature describe the oxidation process of hydrazine due to high interest in the chemical and pharmaceutical industries. This substance is used in many fields, for example in agriculture, as a pesticide, as a pharmaceutical intermediate, water treatment, corrosion protection, textile dyes, and fuel cells. As a consequence, recent activities have been directed towards the development of sensitive and selective analytical methods for the determination of hydrazine [12–14].

In this work, the experimental procedures for the preparation and characterization of a copper hexacyanoferrate film on a modified electrode prepared by the self-assembly of a 3-mercaptopropyltrimethoxysilane on gold surface are reported. The sol–gel processing method was used to prepare the mercaptopropyl-modified electrode, as described for similar systems [15–18]. The copper hexacyanoferrate (CuHCF) film thickness was carefully controlled using a layer-by-layer technique to achieve an ideal film distribution on the surface and, thus, more efficient mass transport on the electrode [19–21]. The electrochemical response of the copper hexacyanoferrate film and its thickness on the substrate surface were investigated by cyclic voltammetry. The film morphology at the electrode surface was studied by scanning electron microscopy. Electrochemical impedance spectroscopy was used to determine the value of the charge transfer resistance.

## Experimental

### Preparation of mercaptopropyl modified gold electrode

The Au working electrode was polished with alumina slurry and sonicated in water/ethanol (1:1 v/v) for 15 min. The polished Au electrode was then electrochemically cleaned by

cycling the potential between 0.2 and 1.5 V in 0.05 mol L<sup>-1</sup> H<sub>2</sub>SO<sub>4</sub> at a scan rate of 0.1 V s<sup>-1</sup> for 10 min to obtain a cyclic voltammogram characteristic of a clean Au electrode.

The sol–gel network was prepared using a 20 mmol L<sup>-1</sup> 3-mercaptopropyltrimethoxysilane (Acros Organics) ethanolic solution at a pH adjusted to 3.0 with HCl. The cleaned Au electrode was modified by immersion in this solution for 30 min. The resulting modified Au electrode was then thoroughly washed with water to remove any residue.

### Preparation of copper hexacyanoferrate film on modified gold electrode

To control the thickness of the copper hexacyanoferrate film, the obtained 3-mercaptopropyltrimethoxysilane modified gold electrode (AuS) was immersed in a 20 mmol L<sup>-1</sup> copper chloride aqueous solution and then washed with water to remove the physically adsorbed metal ions. The electrode was then put into contact with a 20 mmol L<sup>-1</sup> potassium hexacyanoferrate aqueous solution to form a film of copper hexacyanoferrate complex (K<sub>4-2n</sub>Cu<sub>n</sub>[Fe(CN)<sub>6</sub>]) on the surface, hereafter designated as AuS/CuHFC. The effect of the number of immersions in copper and hexacyanoferrate ion were studied from one to six immersions. For the preparations with three and six immersions, the contact time of the electrode with the copper and iron solutions was varied from 5, 10, 20, and 30 min. With the preparation conditions established, the prepared electrodes with three and six immersions for 20 min each were used for the electrochemical studies and, hereafter, designated as AuS/CuHCF3 and AuS/CuHCF6, respectively.

### Scanning electron microscopy

The AuS/CuHCF3 and AuS/CuHCF6 modified electrodes prepared on gold wires were fixed onto an aluminum support with double-sided tape and coated with a layer of Au (ca. 15 nm) by a BalTec SCD 050 Sputter Coater apparatus (60 mA current for 60 s). Scanning electron microscopy (SEM) analyses were carried out on a JSM 5900LV low-vacuum microscope operating at an accelerating voltage of 25 kV while utilizing the secondary electron detector.

### Electrochemical study

Electrochemical studies were carried out using cyclic voltammetry and electrochemical impedance spectroscopy (EIS) techniques. A three-electrode system consisting of the modified gold working electrode, a saturated calomel reference electrode, and a platinum wire counter electrode was utilized. Impedance experiments were carried out with a frequency range between 100 kHz and 10 mHz and a 10 mV amplitude sinusoidal voltage. The supporting

electrolyte solution for the experiments was  $0.10 \text{ mol L}^{-1}$   $\text{KNO}_3$ . All measurements were taken with an Autolab PGSTAT 30 potentiostat–galvanostat apparatus.

## Results and discussion

### Electrochemical electrode characterization

The modified gold electrode coating was prepared via the self-assembly and condensation of a  $(\text{CH}_3\text{O})_3\text{Si}(\text{CH}_2)_3\text{SH}$  precursor in the presence of water and hydrochloric acid as the condensation catalysts. The copper hexacyanoferrate film was prepared with consecutive immersions in the solutions of the complex components. Solid metal hexacyanometalates are very useful as ion-selective materials, as the redox reactions of lattice metal ions are accompanied by a reversible exchange of cations between the electrolyte solution and interstitial holes of the solid compound. Figure 1 shows a schematic representation of the idealized cubic structure for the first layer [22]. The hexacyanoferrate (II) ion is attached to the electrode surface by a well described covalent interaction between the metal and the free SH groups at the siloxane network [1, 5, 10].

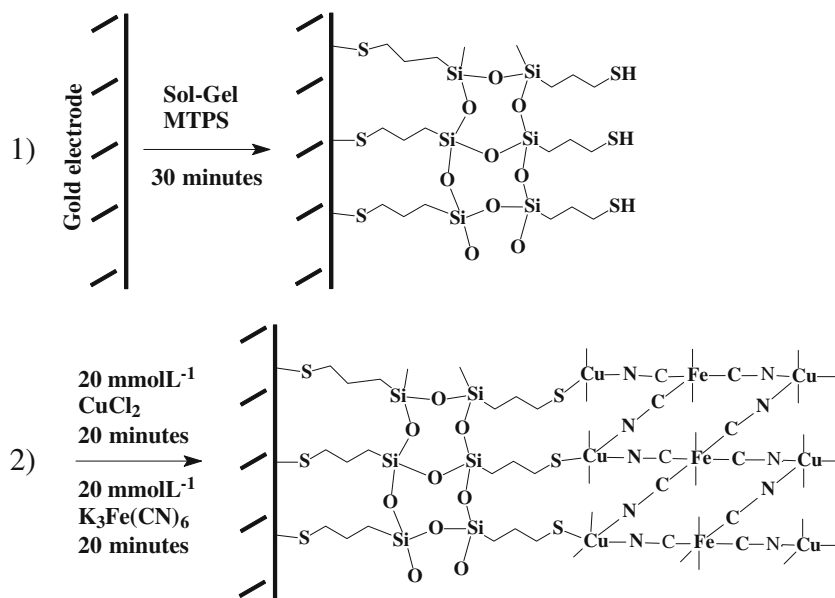
Figure 2 shows the cyclic voltammograms of the AuS/CuHCF modified gold electrode in  $0.10 \text{ mol L}^{-1}$   $\text{KNO}_3$  solution at a scan rate of  $50 \text{ mV s}^{-1}$ . The results showed the iron oxidation peak at approximately  $0.67 \text{ V}$  and the respective reduction peak at  $0.62 \text{ V}$ . The current density reveals a direct relation with the number of immersions as expected, indicating an increase of the copper hexacyanoferrate film thickness after each immersion. The redox process at  $0.90 \text{ V}$  can be attributed to the reduction of free

hexacyanoferrate ion, which remains at the surface after washing the electrode [23].

To control the copper hexacyanoferrate film thickness, the immersion time was studied with two different numbers of immersions at the same conditions. The results are presented in Fig. 3. Current density shows a proportional increase with immersion time. Considering the maximum density current at the iron oxidation peak, the hexacyanoferrate film thickness was calculated for the conditions used in the experiment [15, 24], and the results are presented in Table 1. For the AuS/CuHCF3 electrode, the thickness increase occurs mainly at 20 minutes of immersion time, while for the AuS/CuHCF6 electrode the increase occurs at 10 min of immersion time. The time of 20 minutes was chosen because the intention is to achieve the best condition between a lower thickness and good surface recovery. In addition, the thickness difference between the AuS/CuHCF3 and AuS/CuHCF6 at this time is higher for 30 min, which allows a better situation to study the thickness influence on diffusion process and electron transfer. The electrode which was immersed three times presented an adequate thickness, as there was no saturation of the electrode surface, allowing for a more efficient mass transport into the film. The prepared electrodes had long-term stability, as there was no change in the current density after ten to 50 cycles.

Cyclic voltammograms using different supporting electrolytes were obtained to determine the formation of the copper hexacyanoferrate film at the electrode surface. The literature reports on the solution cation effect on the electrochemical behavior of electrodes with hexacyanoferrate films [15, 25]. The cation diffuses into the film to maintain system electroneutrality. When a cation with a high hydrated radius is present in the solution, the

**Fig. 1** Schematic representation of electrode preparation



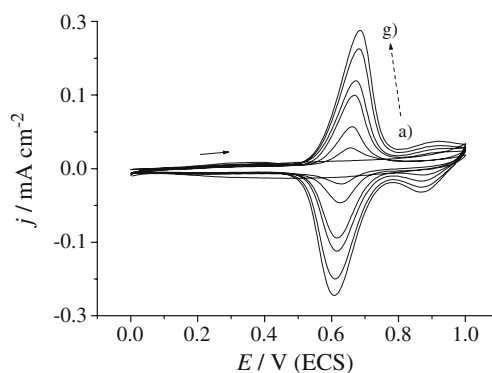


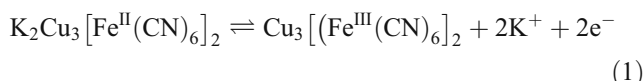
**Fig. 2** Cyclic voltammograms of modified gold electrode AuS/CuHCF, in  $0.10 \text{ mol L}^{-1} \text{ KNO}_3$  solution, with a scan rate of  $50 \text{ mV s}^{-1}$ . *a* clean gold electrode and *b* first, *c* second, *d* third, *e* fourth, *f* fifth, and *g* sixth immersions. Immersion time: 20 min

voltammogram presents broader iron oxidation-reduction peaks. This can be explained by a lower diffusion velocity of the supporting electrolyte cation into the CuHCF film and the incorporation of cation into the hexacyanoferrate film, resulting in a mixture of complex with different stoichiometric. This leads to different iron oxidation-reduction potentials and the subsequent overlapping of the reactions. The redox reaction at the electrode surface is

**Table 1** Thickness film data for the AuS/CuHCF modified electrodes

Time in minutes	Film thickness/nm	
	AuS/CuHCF3	AuS/CuHCF6
5	2.9	7.4
10	4.7	10.4
20	5.6	10.8
30	8.3	11.5

complex and involve the mixture of two compounds,  $\text{Cu}_2[\text{Fe}(\text{CN})_6] / \text{K}_2\text{Cu}[\text{Fe}(\text{CN})_6]$ , which can be represented by  $\text{K}_2\text{Cu}_3[\text{Fe}^{\text{II}}(\text{CN})_6]_2$ . An overall representation can be written as follows [26]:



The cyclic voltammograms for AuS/CuHCF3 and AuS/CuHCF6 obtained with different supporting electrolytes in the solution are presented in Fig. 4. The result shows characteristic electrochemical behavior as described for similar systems, with a broader oxidation-reduction peak and a change of the peak potentials for the electrode with a thicker hexacyanoferrate film (AuS/CuHCF6) [12].

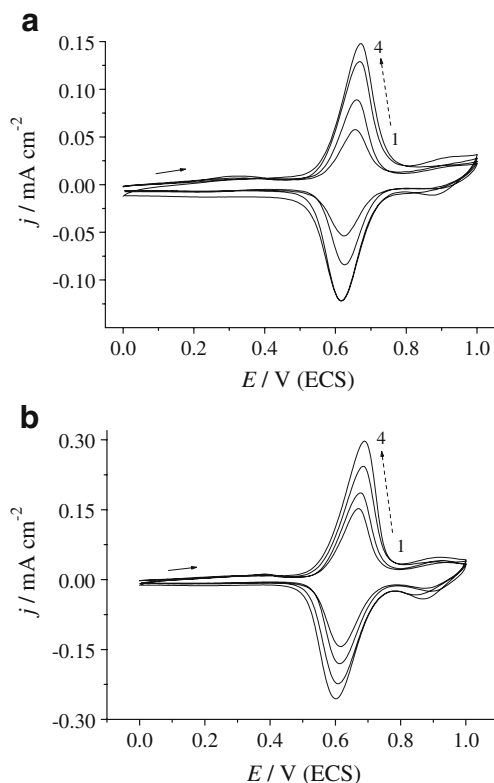


**Fig. 3** Cyclic voltammograms of modified electrode for **a** AuS/CuHCF3 and **b** AuS/CuHCF6 with  $0.10 \text{ mol L}^{-1} \text{ KNO}_3$  support electrolyte. Scan rate was  $50 \text{ mV s}^{-1}$ . Under different immersion time: 1 5 min, 2 10 min, 3 20 min, and 4 30 min

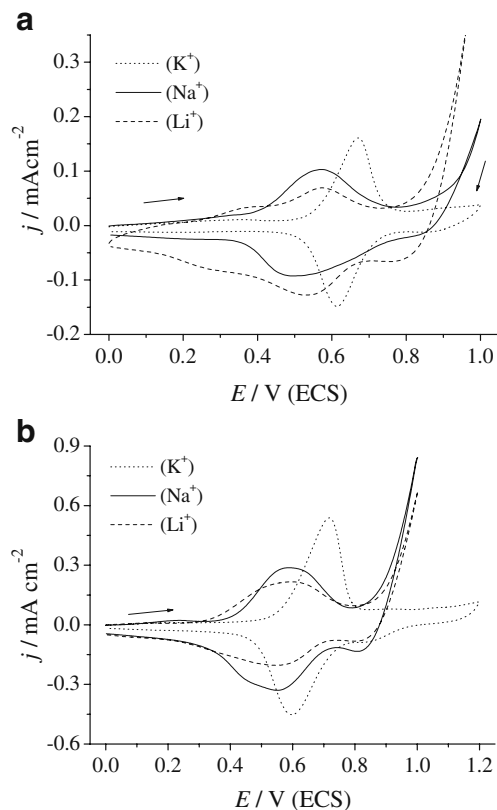


**Fig. 4** Cyclic voltammograms of AuS-CuHCFe modified electrode in a solution of  $0.10 \text{ mol L}^{-1}$  containing  $\text{K}^+$ ,  $\text{Na}^+$ , or  $\text{Li}^+$  (nitrates), for **a** AuS/CuHCF3 and **b** AuS/CuHCF6. Scan rate was  $50 \text{ mV s}^{-1}$

### Copper hexacyanoferrate film on AuS/CuHCF electrode surface

Images obtained by scanning electron microscopy of the electrode surface are presented in Fig. 5. A roughness increase at the electrode surface owing to surface modification of the gold electrode with the mercaptopropyl sol–gel network can be observed (Figs. 5a and b). Figure 5c presents a different morphology at the surface when compared with 5b; this can be attributed to copper hexacyanoferrate film formation. With the magnification used, a surface roughness increase is observed when comparing AuS/CuHCF3 (Fig. 5c) with AuS/CuHCF6 (Fig. 5d), owing to the copper hexacyanoferrate film growth at the electrode surface [15].

### Electrochemical studies

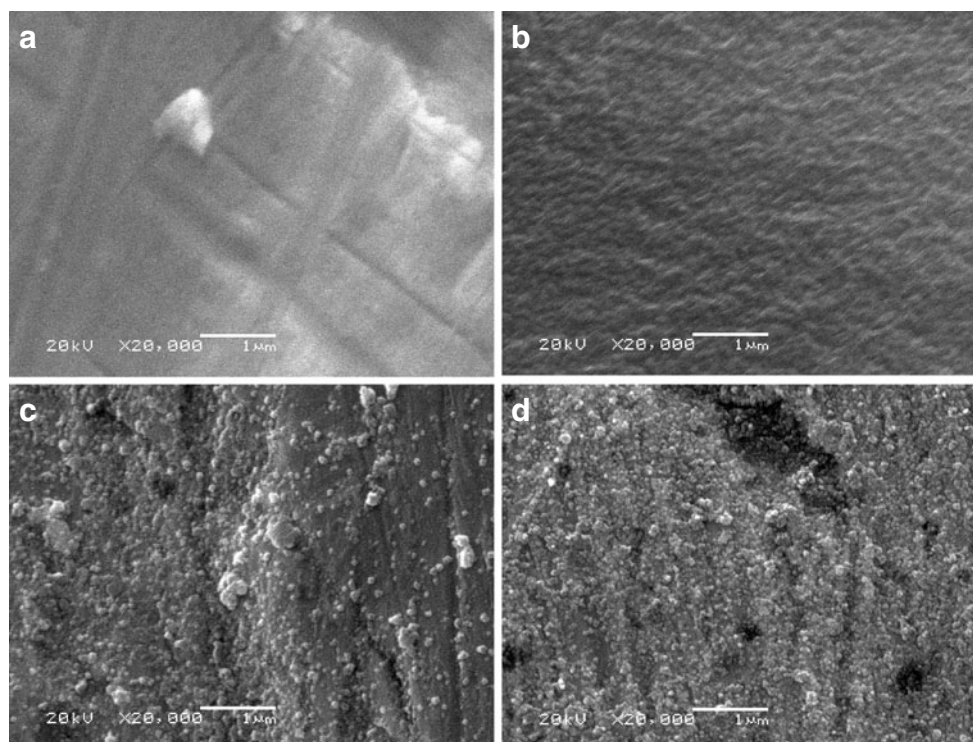
Figure 6 shows the cyclic voltammetry curves for AuS/CuHCF3 (taken as a representative sample) sweeping the potential between 0.0 and 1.0 V with a scan rate between 20 and 500 mV s<sup>-1</sup>. A well-defined redox couple with mid-point potential  $E_m=0.64$  V ( $E_m=(E_{pa}+E_{pc})/2$ , where,  $E_{pa}$  and  $E_{pc}$  are the anodic and cathodic peak potentials, respectively) was observed at 20 mV s<sup>-1</sup> in 0.1 mol L<sup>-1</sup> KNO<sub>3</sub> solution as the supporting electrolyte. With the scan rate increment, the difference potential between the oxidation and reduction pick increased, indicating a quasi-reversible system. A linear relationship between the current density and the square root of the scan rate was observed for AuS/CuHCF3, indicating a

high dependence on counter-ion diffusion at the surface electrode. The electrochemical behavior presented is typical for electrodes with Prussian blue analogs, and the  $E_m$  observed is very similar to those found for copper hexacyanoferrate immobilized on different substrate surfaces [27, 28]. The cyclic voltammograms with an increase of the potential scan rate for the AuS/CuHCF6 electrode presented the same behavior described for AuS/CuHCF3.

To determine the conducting character of the material, i.e., the capacitive and diffusion processes that occur on the surface of the material, EIS measurements were obtained. Figure 7 shows the complex plane impedance plots for AuS/CuHCF6 at (a) OCP potential and (b) iron oxidation potential (0.674 V). The results given in Fig. 7a present a capacitive behavior for all frequency ranges, which is characteristic for systems in chemical equilibrium. Different processes can be observed for measurements obtained at the iron oxidation potential (Fig. 7b). At higher frequency values, electron transfer from iron in the hexacyanoferrate film occurs. A capacitive process can be observed at intermediary frequencies, and the behavior at low frequencies can be attributed to the K<sup>+</sup> diffusion process into the film to maintain electroneutrality of the system [8, 29].

Figure 8 presents the complex plane impedance plot for the AuS/CuHCF3 and AuS/CuHCF6 electrodes. The results obtained show a strong dependence of the charge transfer process on the thickness of the hexacyanoferrate film on the electrode surface. For AuS/CuHCF3, only the diffusion and charge transfer processes can be observed; however, for AuS/

**Fig. 5** Images obtained by SEM of **a** Au, **b** AuS, **c** AuS/CuHCF3, and **d** AuS/CuHCF6. Immersion time: 10 min



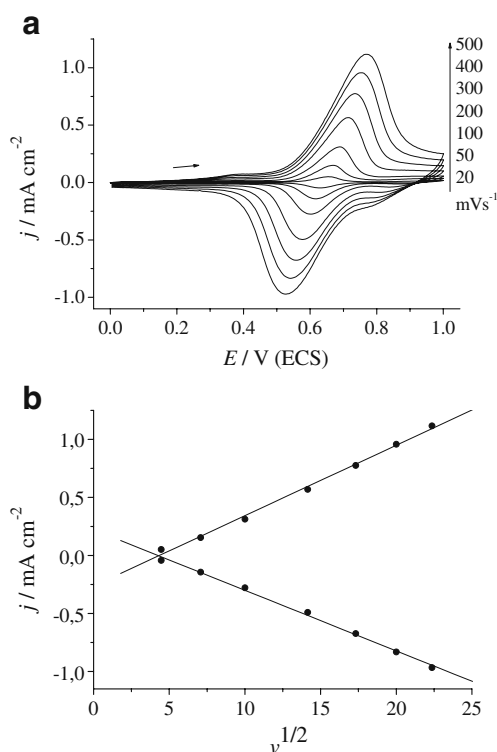


**Fig. 6** **a** Cyclic voltammograms of AuS/CuHCF<sub>3</sub>, supporting electrolyte 0.10 mol L<sup>-1</sup> KNO<sub>3</sub> solution. Scan rate from 20 to 500 mV s<sup>-1</sup>. **b** Plot of the current density versus the square root of scan rate

CuHCF6 an additional capacitive process at intermediary frequencies can be observed. [30]

The electron transfer resistance was determined from the intersection of the semicircle, which can be related to iron oxidation and reduction. The values of electrolyte, polarization and charge transfer resistance obtained for the AuS/CuHCF3 and AuS/CuHCF6 are presented in Table 2.

The small difference in the  $R_s$  values obtained for the prepared electrodes can be attributed to the electrochemical cell arrangement. The  $R_{ct}$  value determined for the AuS/CuHCF6 electrode was higher than that obtained for the AuS/CuHCF3 electrode. This can be attributed to the hexacyanoferrate film thickness on the electrode surface, since the charge transfer process demands the simultaneous diffusion of K<sup>+</sup> into the surface. With these results, it can be concluded that the AuS/CuHCF3 electrode presents the best properties for electrocatalytic studies, since the  $R_{ct}$  is lower than for the AuS/CuHCF6 electrode and diffusion of counter-ions into the hexacyanoferrate film is faster.

#### Electrocatalytic oxidation of hydrazine

To evaluate the potential use of the material as an electrochemical sensor, the electrocatalytic oxidation of

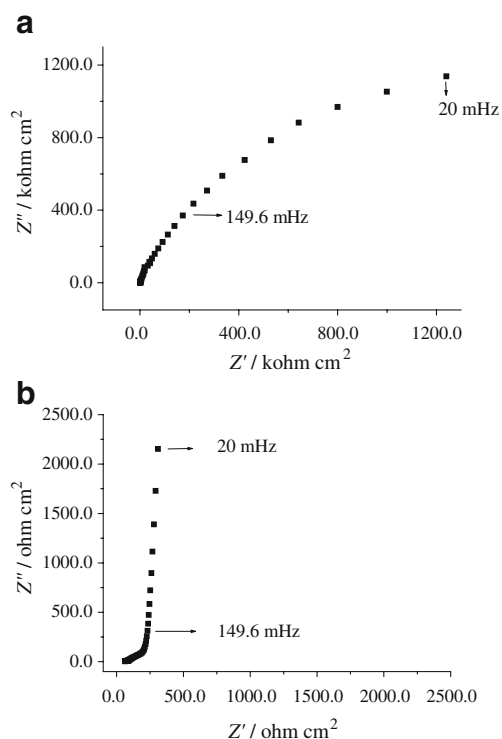


**Fig. 7** Typical complex plane impedance diagram for prepared electrodes. **a** Measurement at OCP potential for AuS/CuHCF<sub>6</sub>. **b** Measurement at iron oxidation potential for AuS/CuHCF<sub>6</sub>. Supporting electrolyte 0.10 mol L<sup>-1</sup> KNO<sub>3</sub> solution

hydrazine was studied. Figure 9 shows the cyclic voltammograms obtained using (a) Au electrode, (b) AuS electrode, and (c) AuS/CuHCF3 modified electrode in the presence of hydrazine at a concentration of  $12.9 \times 10^{-2}$  mol L<sup>-1</sup>. The clean Au electrode reveals a peak associated with hydrazine oxidation. There are no electron transfers after the electrode has been modified with the

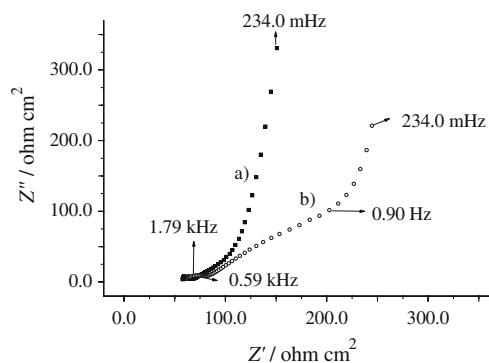


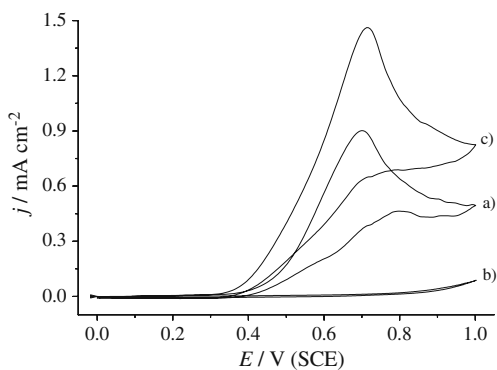
**Fig. 8** Typical complex plane impedance diagram for prepared electrodes. Measurement at iron oxidation potential for *a* AuS/CuHCF<sub>3</sub> and *b* AuS/CuHCF<sub>6</sub>. Supporting electrolyte 0.10 mol L<sup>-1</sup> KNO<sub>3</sub> solution

**Table 2** Values for electrolyte ( $R_s$ ), polarization ( $R_p$ ), and charge transfer resistance ( $R_{ct}$ ), for AuS/CuHCF3 and AuS/CuHCF6 electrodes

	AuS/CuHCF3/ $\Omega$	AuS/CuHCF6/ $\Omega$
$R_s$	52.9 $\pm$ 0.3	59.2 $\pm$ 0.3
$R_p$	72.5 $\pm$ 0.3	87.5 $\pm$ 0.3
$R_{ct}$	19.6 $\pm$ 0.6	27.9 $\pm$ 0.5

mercaptopropyl film. An increase of the anodic current density of 0.6 mA cm<sup>-2</sup> at ~0.7 V was observed for the AuS/CuHCF3 electrode. The cyclic voltammogram (9c) do not show the iron reduction peak because the hydrazine present in solution diffuses toward the electrode and reduces the iron (III) produced electrochemically. An increase of current density on oxidation peak can be observed during the anodic sweep, indicating that the immobilized copper hexacyanoferrate film promotes a higher electrocatalysis rate for hydrazine oxidation at the electrode surface [31].

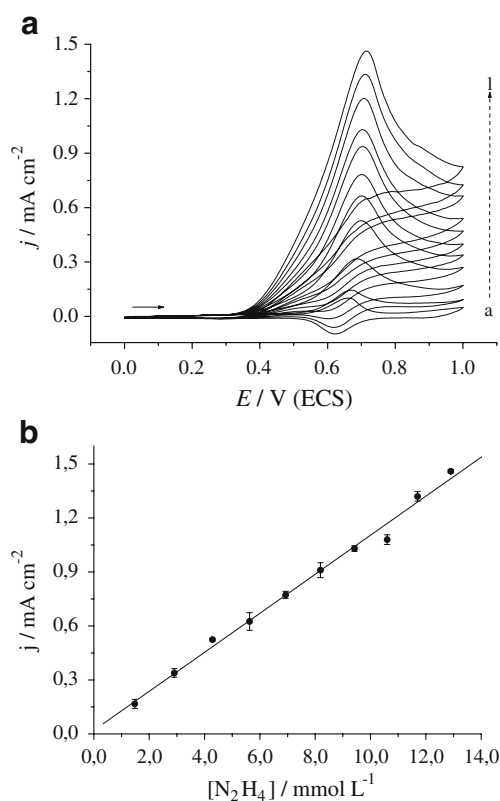
Figure 10a shows the cyclic voltammograms obtained by cycling the potential between 0.0 and 1.0 V in different concentrations of hydrazine. The peak current density around 0.70 V, which increases with successive hydrazine additions, can be assigned to the hydrazine electrooxidation process at the solid–solution interface. A linear correlation for hydrazine concentrations between  $1.48 \times 10^{-4}$  and  $1.29 \times 10^{-3}$  mol L<sup>-1</sup> is observed with a correlation coefficient of 0.9960. The detection limit has been obtained from three times the standard deviation of the blank per the slope of calibration curve [32]. The value was  $7.4 \times 10^{-4}$  mol L<sup>-1</sup>, a good sensitivity when compared to similar systems [29].

**Fig. 9** Cyclic voltammograms of *a* Au, *b* AuS, and *c* AuS/CuHCF3 modified electrode, in a solution of 12.9 mmol L<sup>-1</sup> hydrazine, supporting electrolyte 0.10 mol L<sup>-1</sup> KNO<sub>3</sub> solution, and scan rate of 50 mV s<sup>-1</sup>

## Conclusion

A simple surface modification was achieved with the self-assembly of silane at the gold electrode surface. The methodology of producing this electrode is very simple and reproducible. The immersion of AuS into the reagent solutions resulted in a well-structured copper hexacyanoferrate film on the electrode surface, as indicated by cyclic voltammetry studies. The complex is not leached from the matrix surface when immersed in electrolyte solutions and submitted to electrochemical studies, probably due to the strong bond between the metal and sulfur.

The EIS results showed that the copper hexacyanoferrate film thickness was successfully tuned to obtain an optimized condition for electron transfer, since they indicated that the oxidation/reduction reaction process in the AuS/CuHCF3 system occurred with a lower charge transfer resistance than for the AuS/CuHCF6 electrode. Considering the high stability of the material, the system may be useful in the electroanalytical determination of hydrazine.

**Fig. 10** **a** Cyclic voltammograms of AuS-CuHCFe modified electrode in 0.10 mol L<sup>-1</sup> KNO<sub>3</sub> solution, with different hydrazine concentrations: *a* 0 mmol L<sup>-1</sup>, *b* 1.48 mmol L<sup>-1</sup>, *c* 2.91 mmol L<sup>-1</sup>, *d* 4.29 mmol L<sup>-1</sup>, *e* 5.63 mmol L<sup>-1</sup>, *f* 6.93 mmol L<sup>-1</sup>, *g* 8.19 mmol L<sup>-1</sup>, *h* 9.42 mmol L<sup>-1</sup>, *i* 10.6 mmol L<sup>-1</sup>, *j* 11.7 mmol L<sup>-1</sup>, and *l* 12.9 mmol L<sup>-1</sup>. Scan rate from 50 mV s<sup>-1</sup>. **b** Plot of the current density versus hydrazine concentration

**Acknowledgments** F. L. P. thanks FAPEMIG for post-doctoral fellowship (CEX 00202/08). A.M.S.L. is indebted to FAPEMIG (CEX APQ-3716-5.02/07) and Y.G. to FAPESP for financial support. The authors are also indebted to Prof. Claudia Torres for manuscript revision.

## References

- Wang F, Wang J, Chen H, Dong S (2007) Assembly process of CuHCF/MPA multilayers on gold nanoparticles modified electrode and characterization by electrochemical SPR. *J Electroanal Chem* 600:265–274
- Bilewicz R, Witomski J, Van der Heyden A, Tagu D, Palin B, Rogalska E (2001) Modification of electrodes with self-assembled hydrophobin layers. *J Phys Chem B* 105:9772–9777
- Ricci F, Palleschi G (2005) Sensor and biosensor preparation, optimisation and applications of Prussian Blue modified electrodes. *Biosens Bioelectron* 21:389–407
- Bharathi S, Nogami M, Ikeda S (2001) Layer by layer self-assembly of thin films of metal hexacyanoferrate multilayers. *Langmuir* 17:7468–7471
- Shen Y, Wu T, Zhang Y, Li J (2005) Comparison of two-typed (3-mercaptopropyl)trimethoxysilane-based networks on Au substrates. *Talanta* 65:481–488
- Piwonski I, Grobelny J, Cichomski M, Celichowski G, Rogowski J (2005) Investigation of 3-mercaptopropyltrimethoxysilane self-assembled monolayers on Au(111) surface. *Appl Surf Sci* 242:147–153
- Sibottier E, Sayen S, Gaboriaud F, Walcarius A (2006) Factors affecting the preparation and properties of electrodeposited silica thin films functionalized with amine or thiol groups. *Langmuir* 22:8366–8373
- Yang G, Shen Y, Wang M, Chen H, Liu B, Dong S (2006) Copper hexacyanoferrate multilayer films on glassy carbon electrode modified with 4-aminobenzoic acid in aqueous solution. *Talanta* 68:741–747
- de Tacconi NR, Rajeshwar K, Lezna RO (2003) Metal Hexacyanoferrates: electrosynthesis, in situ characterization, and applications. *Chem Mater* 15:3046–3062
- Cheng WL, Dong SJ, Wang EK (2003) Site-selective self-assembly of MPA-bridged CuHCF multilayers on APTMS-supported gold colloid electrodes. *Chem Mater* 15:2495–2501
- Pauliukaite R, Hocevar SB, Hutton EA, Ogorevc B (2008) Novel electrochemical microsensor for hydrogen peroxide based on iron-ruthenium hexacyanoferrate modified carbon fiber electrode. *Electroanalysis* 20:47–53
- Prabakar SJR, Narayanan SS (2008) Amperometric determination of hydrazine using a surface modified nickel hexacyanoferrate graphite electrode fabricated following a new approach. *J Electroanal Chem* 617:111–120
- Salimi A, Miranzadeh L, Hallaj R (2008) Amperometric and voltammetric detection of hydrazine using glassy carbon electrodes modified with carbon nanotubes and catechol derivatives. *Talanta* 75:147–156
- Chen SM, Wu MH, Thangamuthu R (2008) Preparation, characterization, and electrocatalytic properties of cobalt oxide and cobalt hexacyanoferrate hybrid films. *Electroanalysis* 20:178–184
- Marafon E, Lucho AMS, Francisco MSP, Landers R, Gushikem Y (2006) Thin film of copper hexacyanoferrate dispersed on the surface of a conducting carbon ceramic material, SiO<sub>2</sub>/ZrO<sub>2</sub>/C-graphite: Characteristics and electrochemical studies. *J Braz Chem Soc* 17:1605–1611
- Pissetti FL, Francisco MSP, Landers R, Gushikem Y (2007) Phosphoric acid adsorbed on silica-ceria matrix obtained by sol-gel method: Studies of local structure, texture and acid property. *J Braz Chem Soc* 18:976–983
- Lucho AMS, Pissetti FL, Gushikem Y (2004) Al<sub>2</sub>O<sub>3</sub>-coated 3-N-propylpyridinium chloride silsesquioxane polymer film: preparation and electrochemical property study of adsorbed cobalt tetrasulfophthalocyanine. *J Colloid Interface Sci* 275:251–256
- Fujiwara ST, Pessoa CA, Gushikem Y (2003) Hexacyanoferrate ion adsorbed on propylpyridiniumsilsesquioxane polymer film-coated SiO<sub>2</sub>/Al<sub>2</sub>O<sub>3</sub>: use in an electrochemical oxidation study of cysteine. *Electrochim Acta* 48:3625–3631
- Baioni AP, Vidotti M, Fiorito PA, Ponzio EA, de Torresi SIC (2007) Synthesis and characterization of copper hexacyanoferrate nanoparticles for building up long-term stability electrochromic electrodes. *Langmuir* 23:6796–6800
- Wu BY, Hou SH, Yu M, Qin X, Li S, Chen Q (2009) Layer-by-layer assemblies of chitosan/multi-wall carbon nanotubes and glucose oxidase for amperometric glucose biosensor applications. *Mater Sci Eng C-Biomim Supramol Syst* 29:346–349
- Ou CF, Chen SH, Yuan R, Chai YQ, Zhong X (2008) Layer-by-layer self-assembled multilayer films of multi-walled carbon nanotubes and platinum-Prussian blue hybrid nanoparticles for the fabrication of amperometric immunosensor. *J Electroanal Chem* 624:287–292
- Kahlert H, Retter U, Lohse H, Siegler K, Scholz F (1998) On the determination of the diffusion coefficients of electrons and of potassium ions in copper(II) hexacyanoferrate(II) composite electrodes. *J Phys Chem B* 102:8757–8765
- Karyakin AA (2001) Prussian Blue and its analogues: electrochemistry and analytical applications. *Electroanalysis* 13:813–819
- Siperko LM, Kuwana T (1983) Electrochemical and spectroscopic studies of metal hexacyanometalate films. 1. Cupric hexacyanoferrate. *J Electrochem Soc* 130:396–402
- Prabakar SJR, Narayanan SS (2007) Amperometric determination of paracetamol by a surface modified cobalt hexacyanoferrate graphite wax composite electrode. *Talanta* 72:1818–1827
- Rutkowska IA, Stroka J, Galus Z (2008) Electrochemical properties of modified copper-thallium hexacyanoferrate electrode in the presence of different univalent cations. *Electrochim Acta* 53:3870–3878
- Chen SM, Chan CM (2003) Preparation, characterization, and electrocatalytic properties of copper hexacyanoferrate film and bilayer film modified electrodes. *J Electroanal Chem* 543:161–173
- Makowski O, Stroka J, Kulesza PJ, Malik MA, Galus Z (2002) Electrochemical identity of copper hexacyanoferrate in the solid-state: evidence for the presence and redox activity of both iron and copper ionic sites. *J Electroanal Chem* 532:157–164
- Siperko LM, Kuwana T (1987) Electrochemical and spectroscopic studies of metal hexacyanometalate films. 3. Equilibrium and kinetic-studies of cupric hexacyanoferrate. *Electrochim Acta* 32:765–771
- de Tacconi NR, Rajeshwar K, Lezna RO (2006) Electrochemical impedance spectroscopy and UV-vis reflectance spectroelectrochemistry of cobalt hexacyanoferrate films. *J Electroanal Chem* 587:42–55
- Abbaspour A, Kamyabi MA (2005) Electrocatalytic oxidation of hydrazine on a carbon paste electrode modified by hybrid hexacyanoferrates of copper and cobalt films. *J Electroanal Chem* 576:73–83
- Analytical Methods Committee (1987) Recommendations for the definition, estimation and use of the detection limit. *Analyst* 112:199–204